Annals of Nuclear Medicine Vol. 17, No. 7, 541–548, 2003

Comparison of myocardial fatty acid metabolism with left ventricular function and perfusion in cardiomyopathies: by ^{123}I-BMIPP SPECT and ^{99m}Tc-tetrofosmin electrocardiographically gated SPECT

Chunlei ZHAO,* Noriyuki SHUKE,* Atsutaka OKIZAKI,* Wakako YAMAMOTO,* Junichi SATO,*** Yukio ISHIKAWA,*** Takafumi OHTA,** Naoyuki HASEBE,** Kenjiro KIKUCHI** and Tamio ABURANO*

**Department of Radiology, **First Department of Internal Medicine, and ***Section of Radiology, Asahikawa Medical College and Hospital*

Objective: To investigate myocardial fatty acid metabolism and its relationship with left ventricular (LV) function and perfusion in hypertrophic cardiomyopathy (HCM) and dilated cardiomyopathy (DCM). ***Methods:*** Thirty-nine patients with cardiomyopathies (58 ± 14 y), comprising 15 DCM and 24 HCM, and 9 age-matched healthy controls were studied with ^{123}I-15-(*p*-iodophenyl)-3-(*R,S*)-methylpentadecanoic acid (BMIPP) and ^{99m}Tc-tetrofosmin (TF) electrocardiographically gated SPECT. As parameters of myocardial fatty acid metabolism, the heart-to-mediastinum ratio (H/M) and global washout of BMIPP were calculated from early and delayed planar images, while regional BMIPP uptake and washout were calculated from SPECT. In TF study, the H/M (H/M-TF) and LV ejection fraction (LVEF) were calculated as global parameters of perfusion and function, while regional TF uptake and wall thickening index were calculated as regional parameters of perfusion and function using the Quantitative Gated SPECT software. The differences in the parameters and the correlations between the parameters from the 2 studies were investigated by one-way ANOVA and multiple linear regression analysis. ***Results:*** BMIPP uptake was decreased ($p < 0.05$), and its washout was increased ($p < 0.05$) in DCM and HCM. In multiple linear regression analysis, global BMIPP parameters showed no significant correlation with LVEF ($p > 0.05$), but showed a significant correlation with H/M-TF ($p < 0.05$) in DCM and HCM. According to the partial correlation coefficient, early H/M was the only significant factor ($p < 0.05$) for predicting H/M-TF in DCM and HCM. Multiple linear regression analysis on regional parameters showed regional BMIPP parameters had no correlation with regional function ($p > 0.05$) but had a significant correlation with regional perfusion ($p < 0.0001$) in DCM. In HCM, regional BMIPP parameters showed significant multiple linear correlations with both regional function ($p < 0.005$) and perfusion ($p < 0.0001$). According to the partial correlation coefficients, delayed regional BMIPP uptake was the most significant factor for predicting regional function in HCM, while early regional BMIPP uptake was the only or the most significant factor for predicting regional perfusion in DCM and HCM, respectively. ***Conclusion:*** In DCM, BMIPP uptake and washout could not reflect LV function. In HCM, regional delayed BMIPP uptake might be useful for evaluating regional function. In DCM and HCM, early BMIPP uptake might be largely determined by myocardial perfusion.

Key words: hypertrophic cardiomyopathy, dilated cardiomyopathy, ^{123}I-15-(*p*-iodophenyl)-3-(*R,S*)-methylpentadecanoic acid, ^{99m}Tc-tetrofosmin, gated myocardial SPECT

Received May 20, 2003, revision accepted July 25, 2003.

For reprint contact: Chunlei Zhao, M.D., Department of Radiology, Asahikawa Medical College, 2–1 Midorigaoka-Higashi, Asahikawa 078–8510, JAPAN.

E-mail: zhaocl@asahikawa-med.ac.jp

INTRODUCTION

CARDIAC IMAGING using radio-labeled fatty acids has been used for evaluating myocardial fatty acid metabolism

because free fatty acids are major energy sources for myocardium under normal aerobic conditions.[1,2] Among the available radio-labeled fatty acid compounds, ^{123}I-15-(*p*-iodophenyl)-3-(*R,S*)-methylpentadecanoic acid (BMIPP) is particularly suitable for single-photon emission computed tomography (SPECT) since its prolonged myocardial retention is appropriate for the longer data acquisition periods required for tomographic imaging.[3,4]

In healthy subjects, the distribution of BMIPP in myocardium is as homogeneous as that of ^{201}Tl.[5] In contrast, in ischemic myocardial disease and cardiomyopathy, the distribution of BMIPP is inhomogeneous and is frequently discordant with those of blood flow tracers of ^{201}Tl or ^{99m}Tc-labeled perfusion agents.[6–11] To evaluate the kinetics of BMIPP in myocardium, BMIPP washout rate has usually been used. However, its clinical significance is still controversial. In canine models of ischemic heart disease, the washout in early phase that could reflect the back diffusion of non-metabolized fatty-acid was increased, and the washout in delayed phase that could reflect the myocardial fatty-acid utilization was decreased.[12,13] In hypertrophic cardiomyopathy (HCM), the washout in delayed phase was increased.[14] Studies concerning the relationship between myocardial fatty acid metabolism and LV function in ischemic heart disease revealed that uptake and washout of BMIPP might be correlated with LV function.[15,16] In cardiomyopathies, no consensus has been reached, with some researchers reporting that BMIPP uptake was related to LV function,[5,17,18] while others suggested that abnormalities detected by BMIPP imaging might be independent of LV function as well as perfusion.[19] Therefore, to further understand the myocardial fatty acid metabolism and its relationship with LV function and perfusion in cardiomyopathies, we preformed the present study in a group of patients with dilated cardiomyopathy (DCM) and HCM.

Electrocardiographically (ECG) gated SPECT with ^{99m}Tc-tetrofosmin (TF) and the quantitative gated SPECT (QGS) software were applied to analyze LV perfusion and function simultaneously. This approach could make it easier to compare regional BMIPP uptake or washout with LV perfusion or function on a myocardial segment-by-segment basis.

MATERIALS AND METHODS

Subjects

The study was carried out in 39 patients with cardiomyopathies (mean age, 58 ± 14 y; age range, 15–76 y), including 15 patients with DCM and 24 patients with HCM, and 9 age-matched healthy controls (mean age, 53 ± 17 y; age range, 17–73 y). The diagnosis of HCM and DCM was based on the symptom, history, echocardiographic demonstration of hypertrophic or dilated left ventricle without other cardiac or systemic causes, and histological abnormalities in endocardial biopsy. None of the patients has obvious coronary stenosis (≥50%) on cardiac angiography. Patients with diabetes mellitus, uncontrolled systemic hypertension, cardiac sarcoidosis, and Parkinson's disease were excluded from the study. ^{123}I-BMIPP SPECT and ^{99m}Tc-TF ECG gated SPECT were performed on all subjects within 2 weeks without any medical intervention. All patients gave their informed consent to participate before the study.

Radiopharmaceuticals

^{123}I-BMIPP (Cardiodine; 111 MBq/0.03–0.1 mg) was purchased from Nihon Medi-Physics (Nishinomiya, Japan). ^{99m}Tc-TF was prepared using a kit vial of tetrofosmin (Myoview; Nihon Medi-Physics, Nishinomiya, Japan) and freshly eluted ^{99m}Tc-pertechnetate from ^{99m}Tc generator system (Ultra-TechneKow, Daiichi Radioisotope Laboratory, Tokyo, Japan).

Imaging Protocol

Patients were fasted on the day of the BMIPP study and continued to fast until the study was completed. We performed early and delayed BMIPP imaging using a single-head rotating gamma camera equipped with a low energy general-purpose collimator (RC-135E; Hitachimedico, Tokyo, Japan). Early imaging began 15 min after intravenous injection of 111 MBq of ^{123}I-BMIPP. Before SPECT data acquisition, an anterior chest planar image was acquired for 300 s in a 128 × 128 matrix. Immediately after planar imaging, 32 projection images were obtained in a 64 × 64 matrix for 40 s each, with a 180° rotation and an energy window of 10% centered at 160 keV. Delayed planar imaging and SPECT imaging were performed 4 h after the injection under the same acquisition conditions as used in the early imaging.

For ECG gated TF SPECT, we used a triple-head rotating gamma camera equipped with a low-energy high-resolution collimator (GCA-9300A/DI; Toshiba Medical, Tokyo, Japan). Sixty projection images were obtained using the R wave on electrocardiography as a trigger of acquisition in a 64 × 64 matrix for 30 s each, over 360°, with an energy window of 10% centered at 140 keV at 60 min after an intravenous injection of 740 MBq of ^{99m}Tc-TF. Each image was partitioned into 8 or 16 frames per cardiac cycle.

Reconstruction was done without attenuation and scatter correction by a filtered back-projection algorithm for the BMIPP and TF studies. After preprocessing with a Butterworth filter (cutoff frequency, 0.44 cycle/cm; power factor, 8), transaxial images were reconstructed with a ramp filter. Long- and short-axial slices were then produced by axial reorientation.

Data Processing

On the anterior planar BMIPP images, regions of interest (ROIs) were drawn over the whole heart and upper mediastinum. Using the counts in the ROIs, the heart-to-

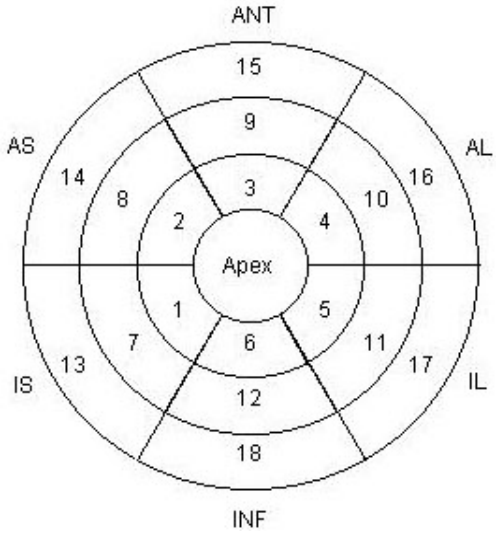

Fig. 1 Diagram of myocardial segments of left ventricle on short-axial plane. IS = inferior septum; AS = anterior septum; ANT = anterior; AL = anterior lateral; IL = inferior lateral; INF = inferior; Segment 1–6, 7–12, and 13–18 correspond to the apical, middle, and basal parts of left ventricle, respectively.

mediastinum count ratio (H/M) and global cardiac washout (GW) of BMIPP were calculated as follows:

$$\text{H/M} = \frac{\text{mean pixel counts of heart ROI}}{\text{mean pixel counts of mediastinum ROI}}$$

$$\text{GW (\%)} = [\text{mean heart pixel counts (early)} - \text{mean heart pixel counts (delayed)}] \times 100/[\text{mean heart pixel counts (early)}],$$

where the H/M from early and delayed images is H/Me and H/Md, respectively. Decay correction was done for calculating GW.

Regional uptake and washout of BMIPP were analyzed on early and delayed short-axial tomographic images. In this analysis for both early and delayed images, after setting the apex and the basal part of LV, count profile of myocardium on each slice was calculated automatically using dedicated software. Then relative regional uptake of BMIPP (RRU-B, %) normalized from the highest counts of LV in each imaging and corresponding regional washout (RW, %) were calculated and displayed on a polar map dividing LV into 18 segments from apex to basal part (Fig. 1). Twelve segments (segment 1 to 12) from apical and middle parts were used for quantitative analysis. To compare regional BMIPP uptake among different individuals, uptake index (BUP) was introduced and calculated as the product of RRU-B and H/M.

$$\text{BUP} = \text{RRU-B} \times \text{H/M}$$

The BUPs of early and delayed images are BUPe and BUPd, respectively. Decay correction was done for calculating RW.

To calculate the H/M of TF (H/M-TF), ROIs of the heart and mediastinum were drawn on an anterior image from the merged non-gated SPECT image because planar imaging was not performed in the TF study:

$$\text{H/M-TF} = \frac{\text{mean pixel counts of heart ROI}}{\text{mean pixel counts of mediastinum ROI}}.$$

Using merged non-gated short axial images, relative regional uptake of TF (RRU-TF, %) normalized by the highest voxel counts was obtained from dedicated software and displayed in the bull's eye map. To compare regional TF uptakes among different individuals, uptake index (UPTF) defined as the product of RRU-TF and H/M-TF was introduced.

$$\text{UPTF} = \text{RRU-TF} \times \text{H/M-TF}$$

Applying the QGS software (QGS 2.0, Cedars-Sinai Medical Center, Los Angeles, CA) to the ECG-gated SPECT images, LV ejection fraction (LVEF) and regional wall thickening (WT) were computed and displayed in the bull's eye maps. Considering that the WT may not be equal throughout the whole LV, normal segmental WT was calculated for every segment as the mean value of the segmental WT of the normal controls. For comparing the WT in the patient without the influence of uneven LV contraction, the WT of the patients were divided by the corresponding normal segmental WT to obtain a ratio, which was defined as wall thickening index (WTI). The WTI indicates to what extent the WT of the patient reduced compared to the normal segmental WT.

The same 12 segments from apex and middle parts of LV as shown in Figure 1 were used for analysis in the TF study.

The parameters from both studies are summarized in Table 1. For testing the reproducibility of the parameters, the values of all the parameters in 5 patients with HCM and 5 patients with DCM were recalculated by the same observer on two occasions and also by a second observer.

Statistical Analysis

One-way ANOVA was applied for comparing the parameters from the BMIPP and TF studies. To determine if the factors were independently related to LV function and perfusion, the parameters from the BMIPP study were examined by multiple linear regression analysis using the Statistica software package (STATISTICA'99 Edition Release 5.5A, StatSoft Inc., Tulsa, OK, USA). Multiple and partial correlation coefficients were calculated. A $p < 0.05$ was considered significant in all tests.

RESULTS

The clinical and echocardiographic data of the patients with DCM and HCM are summarized in Table 2. Of 15 patients with DCM, one had a history of viral myocarditis, one had alcohol addiction, and the other 13 were idiopathic without known primary causes. Of 24 patients with HCM,

Table 1 Global and regional parameters in study

Parameters of MFAM
Global
GW: global % washout of BMIPP
H/Me, H/Md: early and delayed heart-to-mediastinum ratio in BMIPP study
Regional
RW: regional % washout of BMIPP
BUPe, BUPd: early and delayed BMIPP uptake index
Parameters of LV function
Global
LVEF: left ventricular ejection fraction
Regional
WTI: wall thickening index
Parameters of myocardial perfusion
Global
H/M-TF: heart-to-mediastinum ratio in tetrofosmin study
Regional
UPTF: tetrofosmin uptake index

Table 2 Clinical characteristics of the patients with DCM and HCM

Characteristics	Value	
	DCM (n = 15)	HCM (n = 24)
Female/male	1/14	3/21
Age (years)	57.46 ± 12.99	58.67 ± 14.19
Duration of disease (y)	3.76 ± 3.72	5.32 ± 5.70
History of chest pain	0	4 (17%)
History of syncope	3 (20%)	4 (17%)
Episode of heart failure	12 (80%)	4 (17%)
Family history of HCM		3 (13%)
NYHA functional class (I/II/III/IV)	3/8/2/2	20/4/0/0
VT on Holter ECG	5 (33%)	7 (29%)
CTR (%)	53.34 ± 4.72	54.25 ± 6.15
Echocardiogram		
LAD (mm)	43.15 ± 6.44	41.25 ± 7.54
IVS (mm)	8.67 ± 1.23	15.11 ± 4.35
PW (mm)	9.00 ± 1.04	10.90 ± 2.53
LVDd (mm)	61.80 ± 11.32	50.35 ± 4.81
LVDs (mm)	52.21 ± 9.39	31.74 ± 7.45
FS (%)	17.07 ± 6.43	36.98 ± 9.26
Medication		
ACE inhibitors	14 (93%)	17 (71%)
Beta-blockers	11 (73%)	12 (50%)

NYHA: New York Heart Association. CTR: cardiothoracic ratio. VT: ventricular tachycardia. LAD: left artrial dimension. IVS: interventricular septal thickness. PW: posterior wall thickness. LVDd: left ventricular dimension at end-diastole. LVDs: left ventricular dimension at end-systole. FS: fractional shortening. ACE: angiotension-converting enzyme.

two patients with apical hypertrophy (APH) and 2 patients with asymmetric septal hypertrophy (ASH) were in the dilated phase. Of the remaining 20 patients with HCM, 7 had APH, 9 had ASH, 2 had both APH and ASH, and 2 had global hypertrophy.

The intra-observer and inter-observer variation ranged from ±6.1% to ±3.4%, the correlation coefficient between each of the 2 sets of the values of parameters obtained by the same observer or by different observers ranged from 0.87 to 0.95, all with a $p < 0.001$.

Global parameters

The means of global parameters in healthy control, DCM, and HCM are listed in Table 3. LVEF were significantly different among the three categories, in decreasing order of healthy control, HCM, and DCM. H/M-TF and H/Me in HCM were significantly greater than those in DCM, but showed no difference with those in healthy control. H/Md in both HCM and DCM was decreased comparing to healthy control, but no significant difference was found between DCM and HCM. GW in HCM was greater than both healthy control and DCM, but no difference was found between healthy control and DCM. Within the HCM category, LVEF and H/M-TF in the patients of the non-dilated phase were significantly greater than those in patients of the dilated phase.

Regional parameters

Descriptive statistics of regional parameters in the segments of healthy control, DCM, and HCM are listed in Table 4. WTI, BUPe and BUPd were significantly different among the 3 categories, in decreasing order of healthy control, HCM and DCM. RW was also significantly different among the 3 categories, in decreasing order of HCM, DCM and healthy control. UPTF in HCM and healthy control was significantly higher than that in DCM, but no difference was found between healthy control and HCM. Within the HCM category, all parameters except RW showed significant differences between the patients of the dilated phase and those of the non-dilated phase. UPTF and BUPe showed no difference between DCM and dilated-phase HCM.

Correlation among global parameters

The multiple correlation coefficients between the observed values of LVEF and those predicted from the global BMIPP parameters (H/Me, H/Md and GW) were 0.269 ($p = 0.834$) in DCM and 0.389 ($p = 0.338$) in HCM. These values indicated no significant correlations between LVEF and global BMIPP parameters in DCM or HCM.

The multiple correlation coefficients between the observed values of H/M-TF and those predicted from the global BMIPP parameters were 0.722 ($p = 0.038$) in DCM and 0.703 ($p = 0.003$) in HCM. These values indicated significant correlations between H/M-TF and global BMIPP parameters in DCM and HCM. In DCM, the partial correlation coefficients between H/Me, H/Md, GW, and H/M-TF were 0.675 ($p < 0.05$), –0.433 ($p = 0.139$) and 0.081 ($p = 0.792$). In HCM, these values were

Table 3 Global parameters in healthy control, DCM and HCM

Parameter	Healthy control (n = 9)	DCM (n = 15)	HCM		
			Non-DP (n = 20)	DP (n = 4)	Overall (n = 24)
LVEF (%)	73.44 ± 7.73	32.40 ± 13.44*	52.50 ± 9.44*†	41.75 ± 8.69*‡	50.71 ± 10.01*†
H/M-TF	3.28 ± 0.45	2.62 ± 0.39*	3.54 ± 0.28†	2.66 ± 0.11*‡	3.39 ± 0.42†
H/Me	2.27 ± 0.18	2.07 ± 0.25*	2.26 ± 0.19†	2.10 ± 0.08	2.24 ± 0.19†
H/Md	2.10 ± 0.25	1.80 ± 0.25*	1.90 ± 0.20*	1.79 ± 0.22	1.88 ± 0.21*
GW (%)	10.37 ± 3.60	9.56 ± 5.67	15.17 ± 6.31*†	15.20 ± 6.51	15.17 ± 6.20*†

Data are presented as mean ± SD. n: case number. Non-DP: non-dilated phase. DP: dilated phase. LVEF: left ventricular ejection fraction. H/M-TF: heart-to-mediastinum ratio in TF study. H/Me: early heart-to-mediastinum ratio in BMIPP study. H/Md: delayed heart-to-mediastinum ratio in BMIPP study. GW: global washout of BMIPP. *$p < 0.05$ vs. healthy control. †$p < 0.05$ vs. DCM. ‡$p < 0.05$ vs. non-DP.

Table 4 Regional parameters in healthy control, DCM and HCM (mean ± SD)

Parameter	Healthy control (n = 108)	DCM (n = 180)	HCM		
			Non-DP (n = 240)	DP (n = 48)	Overall (n = 288)
WTI	1.00 ± 0.17	0.38 ± 0.19*	0.55 ± 0.20*†	0.45 ± 0.16*†‡	0.54 ± 0.20*†
UPTF	2.74 ± 0.44	2.05 ± 0.41*	2.95 ± 0.39*†	2.11 ± 0.28*‡	2.81 ± 0.49†
RW (%)	11.60 ± 6.60	17.43 ± 9.42*	23.08 ± 9.99*†	21.95 ± 11.50*†	22.89 ± 10.24*†
BUPe	2.05 ± 0.18	1.70 ± 0.32*	1.94 ± 0.30*†	1.70 ± 0.30*‡	1.90 ± 0.32*†
BUPd	1.96 ± 0.25	1.49 ± 0.26*	1.64 ± 0.24*†	1.39 ± 0.33*†‡	1.60 ± 0.27*†

Data are presented as mean ± SD. n: number of the segments. Non-DP: non-dilated phase. DP: dilated phase. WTI: wall thickening index. UPTF: regional tetrofosmin uptake. RW: regional BMIPP washout. BUPe: early regional BMIPP uptake. BUPd: delayed regional BMIPP uptake. *$p < 0.05$ vs. healthy control. †$p < 0.05$ vs. DCM. ‡$p < 0.05$ vs. non-DP.

Table 5 Sample correlation coefficients (r value) between regional parameters

Parameter	WTI		UPTF	
	DCM (n = 180)	HCM (n = 288)	DCM (n = 180)	HCM (n = 288)
RW	0.177*	–0.132*	0.294†	0.156†
BUPe	0.171*	0.016	0.567†	0.481†
BUPd	0.070	0.214†	0.425†	0.328†

n: number of the segments. WTI: wall thickening index. UPTF: regional tetrofosmin uptake. RW: regional BMIPP washout. BUPe: early regional BMIPP uptake. BUPd: delayed regional BMIPP uptake. *$p < 0.05$, †$p < 0.01$.

0.663 ($p < 0.001$), –0.209 ($p = 0.349$) and 0.092 ($p = 0.683$). In both DCM and HCM, H/Me was the only significant predictor for H/M-TF.

Correlation among regional parameters

The multiple correlation coefficients between the observed values of WTI and those predicted from the regional BMIPP parameters (BUPe, BUPd and RW) were 0.201 ($p > 0.05$) in DCM and 0.274 ($p < 0.0001$) in HCM. Thus, the regional BMIPP parameters showed a significant correlation with regional function in HCM. The partial correlation coefficients between BUPe, BUPd, RW, and WTI were –0.168 ($p < 0.005$), 0.240 ($p < 0.0001$) and 0.059 ($p = 0.32$). These values indicated significant correlations of early and delayed regional BMIPP uptake with regional function in HCM. Compared to early regional BMIPP uptake, delayed regional BMIPP uptake showed a better correlation with regional function.

The multiple correlation coefficients between the observed values of UPTF and those predicted from the regional BMIPP parameters (BUPe, BUPd and RW) were 0.573 ($p < 0.0001$) in DCM and 0.505 ($p < 0.0001$) in HCM. These values indicated significant correlations between regional perfusion and regional BMIPP parameters in DCM and HCM. In DCM, the partial correlation coefficients between BUPe, BUPd, RW, and UPTF were 0.283 ($p < 0.0005$), –0.011 ($p = 0.879$) and 0.072 ($p = 0.337$). In HCM, those values were 0.229 ($p < 0.0001$), 0.133 ($p < 0.05$) and 0.172 ($p < 0.005$), respectively. In DCM and HCM, early regional BMIPP uptake showed the only significant or the best correlation with regional perfusion, respectively.

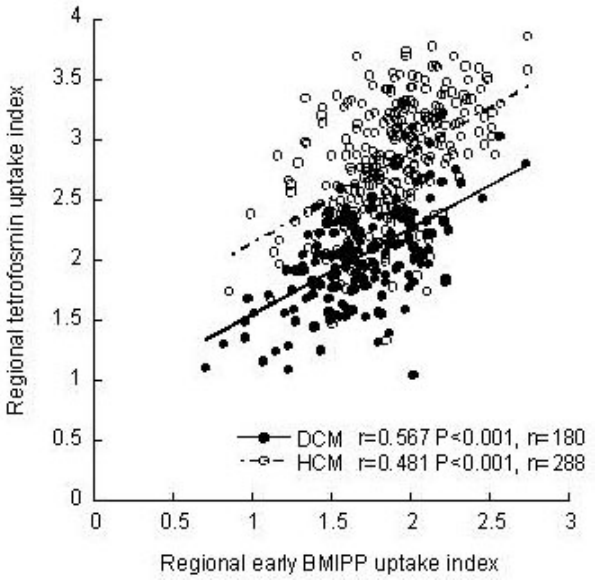

Fig. 2 Correlation between regional early BMIPP uptakes and perfusion in DCM and HCM. n = number of myocardial segments.

Table 5 shows sample correlation coefficients between the parameters in DCM and HCM. The correlation coefficients between UPTF and BUPe were 0.567 ($p < 0.001$) in DCM and 0.481 ($p < 0.001$) in HCM (Fig. 2).

DISCUSSION

Cardiac BMIPP abnormalities, such as heterogeneous distribution, low uptake and abnormal washout, have been revealed in cardiomyopathies.[7,8,14] These abnormalities are thought to reflect abnormal myocardial fatty acid metabolism associated with cardiomyopathy. However, little is known about the relationship between these BMIPP abnormalities and the pathophysiology of cardiomyopathies. In this study, we found that myocardial fatty acid metabolism evaluated from the uptake and washout of BMIPP might not be able to reflect myocardial function in DCM, whereas in HCM, regional delayed BMIPP uptake might be helpful for evaluating regional function.

In non-dilated HCM, regional uptake of TF was even better than that in healthy controls. However, regional function, early and delayed BMIPP uptake were decreased and BMIPP washout was increased compared to those in healthy controls, implying that even if myocardial perfusion dose not decrease in non-dilated HCM, LV function and myocardial fatty acid metabolism may be disordered. DCM was associated with the lowest LV function, TF uptake and BMIPP uptakes except that delayed BMIPP uptake was higher than that of HCM in the dilated phase. These findings in DCM were in concordance with the pathophysiologic characteristics of DCM.[20] Although HCM in the dilated phase had similarly low TF uptake and early BMIPP uptake like DCM, its delayed BMIPP uptake was lower and its BMIPP washout was higher than those of DCM, implying that the kinetics of BMIPP might differ between DCM and HCM.

BMIPP uptake, washout, and their relations with LV perfusion

In HCM and DCM, the distribution of BMIPP may be more heterogeneous than that of blood flow tracer.[7,9–11] In HCM, even in normally contracting hypertrophic myocardium with normal or high perfusion, BMIPP uptake may reduced,[9] suggesting that regional myocardial fatty acid metabolism could alter either independent of perfusion or before any alteration of perfusion in cardiomyopathy.[8] However, Tamaki et al. pointed out that the initial distribution of BMIPP is largely determined by regional myocardial blood flow.[6] In agreement with their view, our results showed that early BMIPP uptake was the only significant factor in DCM and the most significant factor in HCM for predicting LV perfusion, indicating that early BMIPP uptake might be largely dependent on the blood flow in HCM and DCM.

In normal myocardium, retained BMIPP is cleared out slowly and most of the washout is due to α- and β-oxidation metabolites, with only little loss of BMIPP itself.[21] In an animal model of myocardial ischemia at very early phase (8 minutes), BMIPP washout was increased due to the accelerated back-diffusion of non-metabolized BMIPP,[12,13] while BMIPP washout at 3 hr, which could be considered as "late-phase," was decreased.[22] In HCM, on the contrary, BMIPP washout at 3 hr was significantly increased.[14] In agreement with this finding, our results showed that regional BMIPP washout was increased in HCM, as well as in DCM. These results confirmed that the mechanism of BMIPP washout in cardiomyopathies might be different from that in ischemic heart disease.

Relationship of BMIPP uptake and washout with LV function

As an energy substance, free fatty acid may play an important role in maintaining LV function. As a fatty acid compound, BMIPP is instantly extracted from the plasma into the myocardium and is incorporated mainly into the endogenous triglyceride pool.[21,23,24] However, BMIPP could not be easily metabolized by β-oxidation, and its retention as acyl-coenzyme A in myocyte requires ATP.[25] Therefore, the myocardial uptake and retention of BMIPP may not directly indicate fatty acid metabolism but may be acceptable for assessing myocardial fatty acid utilization.[25] Reports regarding the relation between BMIPP uptake and LV perfusion in cardiomyopathy are controversial. Several authors reported that BMIPP uptake might be correlated with LV function in HCM and DCM.[5,17,18] Kobayashi et al., on the contrary, reported that abnormalities detected in BMIPP imaging might be independent of

LV function as well as perfusion in HCM.[19] As for the relation between myocardial BMIPP washout and LV function in cardiomyopathies, little is known. In our study, LVEF showed no correlation with global BMIPP parameters in DCM and HCM. In DCM, regional parameters showed no correlation with regional function either. In HCM, on the other hand, regional delayed BMIPP uptake was found to be the most significant factor for predicting regional function. These results indicated that BMIPP imaging could not evaluate LV function in DCM. However, in HCM, the reduced delayed regional BMIPP uptake might be helpful for reflecting the regional function. It is possible that in the dysfunctional area in HCM, the utilization of fatty acid might be impaired.

Limitations of the study

The TF uptake was used to evaluate the myocardial perfusion in this study although the TF uptake may partly related to energy-dependent processes such as Na^+/H^+ antiporter system, cellular and mitochondrial membrane potentials.[26,27] In cardiomyopathy, metabolic impairment may occur; however, little is known about the influence of such metabolic impairment on the myocardial TF uptake. On the other hand, the TF uptake has been found to correlate closely with blood flow.[28,29] In addition, a study indicated that in ischemic but viable myocardium, only about 29% of the TF uptake reduction could be accounted for as flow-independent in the area of ^{18}F-FDG and TF mismatch,[30] suggesting that the TF uptake may reflect myocardial perfusion to a large extent. Therefore, we adopted TF imaging in the study and believed it could provide proper evaluation of the myocardial perfusion.

The global parameters used in the study were measured from planar images because this was a simple and reproducible way to evaluate the tracer's uptake.[31] However, planar imaging has its own limitations because of the counts of overlying lung.[31] Thus, in the patients whose cardiac uptake of the tracer was decreased significantly, the global washout might largely reflect the washout of overlying lung rather than the heart, and the H/M might be overestimated. Regional uptakes of the tracers were normalized by the H/M values in this study. Although this method was not ideal to evaluate absolute uptake, the normalized regional uptake indexes might be superior to the relative parameters of uptake when the comparison among the individuals was considered. A more accurate index should be sought to lessen this error.

Since the data from the BMIPP and TF studies were acquired separately with different machines, exact matching of the corresponding anatomic sites was impossible. However, all the regional analysis was processed automatically and presented good reproducibility. In addition, since the conditions of reconstruction for both imaging, especially the angles of axial reorientation, were kept as similar as possible, the errors caused by the mismatching might be limited to an acceptable range. We excluded the basal part of the myocardium from the regional analysis because the results from this site appeared quite inaccurate, possibly associated with the difficulty of determining its border even if processed automatically.

CONCLUSION

Our study suggested that myocardial fatty acid metabolism evaluated from the uptake and washout of BMIPP could not reflect LV function in DCM. However, in HCM, regional delayed BMIPP uptake might be useful for evaluating regional function. In both DCM and HCM, early cardiac uptake of BMIPP might be largely determined by myocardial perfusion.

ACKNOWLEDGMENTS

The authors thank Nihon Medi-Physics Co. Ltd. for their cooperation to this study.

REFERENCES

1. Neely JR, Rovetto MJ, Oram JF. Myocardial utilization of carbohydrate and lipids. *Prog Cardiovasc Dis* 1972; 15: 289–329.
2. Zierler KL. Fatty acids as substrates for heart and skeletal muscle. *Circ Res* 1976; 38: 459–463.
3. Goodman MM, Kirsch G, Knapp FF Jr. Synthesis and evaluation of radioiodinated terminal *p*-iodophenyl-substituted alpha- and beta-methyl-branched fatty acids. *J Med Chem* 1984; 27: 390–397.
4. Bax JJ, Knapp FF, Visser FC. Single-photon imaging of myocardial metabolism: the role of iodine-123 fatty acids and fluorine-18 deoxyglucose. In: Murray IPC, Ell PJ, eds. *Nuclear Medicine in Clinical Diagnosis and Treatment*. Edinburgh, U.K.; Churchill Livingstone, 1998: 1497–1501.
5. Shimonagata T, Nishimura T, Uehara T, Hayashida K, Kumita S, Ohno A, et al. Discrepancies between myocardial perfusion and free fatty acid metabolism in patients with hypertrophic cardiomyopathy. *Nucl Med Commun* 1993; 14: 1005–1013.
6. Tamaki N, Kawamoto M, Yonekura Y, Fujibayashi Y, Takahashi N, Konishi J, et al. Regional metabolic abnormality in relation to perfusion and wall motion in patients with myocardial infarction: assessment with emission tomography using an iodinated branched fatty acid analog. *J Nucl Med* 1992; 33: 659–667.
7. Kurata C, Tawarahara K, Taguchi T, Aoshima S, Kobayashi A, Yamazaki N, et al. Myocardial emission computed tomography with iodine-123-labeled beta-methyl-branched fatty acid in patients with hypertrophic cardiomyopathy. *J Nucl Med* 1992; 33: 6–13.
8. Kurata C, Kobayashi A, Yamazaki N. Dual tracer autoradiographic study with thallium-201 and radioiodinated fatty acid in cardiomyopathic hamsters. *J Nucl Med* 1989; 30: 80–87.
9. Takeishi Y, Chiba J, Abe S, Tonooka I, Komatani A, Tomoike H. Heterogeneous myocardial distribution of iodine-123 15-(*p*-iodophenyl)-3-*R*,*S*-methylpentadecanoic acid (BMIPP) in patients with hypertrophic cardiomyopa-

thy. *Eur J Nucl Med* 1992; 19: 775–782.
10. Shimizu M, Yoshio H, Ino H, Taki J, Nakajima K, Bunko H, et al. Myocardial scintigraphic study with ^{123}I 15-(*p*-iodophenyl)-3(*R,S*)-methylpentadecanoic acid in patients with hypertrophic cardiomyopathy. *Int J Cardiol* 1996; 54: 51–59.
11. Narita M, Kurihara T. Fatty acid metabolism in patients with idiopathic dilated cardiomyopathy: characteristics and prognostic implications. *J Cardiol* 1995; 25: 223–231.
12. Hosokawa R, Nohara R, Fujibayashi Y, Okuda K, Ogino M, Hata T, et al. Myocardial kinetics of iodine-123-BMIPP in canine myocardium after regional ischemia and reperfusion: implications for clinical SPECT. *J Nucl Med* 1997; 38: 1857–1863.
13. Hosokawa R, Nohara R, Fujibayashi Y, Okuda K, Ogino M, Hirai T, et al. Myocardial metabolism of ^{123}I-BMIPP in a canine model with ischemia: implications of perfusion-metabolism mismatch on SPECT images in patients with ischemic heart disease. *J Nucl Med* 1999; 40: 471–478.
14. Chen SL, Uehara T, Morozumi T, Yamagami H, Kusuoka H, Nishimura T. Myocardial metabolism of ^{123}I-BMIPP in patients with hypertrophic cardiomyopathy: assessment by radial long-axis SPET. *Nucl Med Commun* 1995; 16: 336–343.
15. Matsunari I, Saga T, Taki J, Akashi Y, Wakasugi T, Hirai JI, et al. Relationship between various parameters derived from ^{123}I-labelled beta-methyl-branched fatty acid whole-body scintigraphy and left ventricular ejection fraction in patients with ischaemic heart disease. *Nucl Med Commun* 1994; 15: 685–689.
16. Abe M, Joh T, Hara Y, Hashida K, Koyama Y, Kazatani Y. Evaluation of myocardial damage using ^{123}I-BMIPP imaging in patients with vasospastic angina. *KAKU IGAKU (Jpn J Nucl Med)* 1996; 33: 599–606.
17. Shimizu M, Ino H, Okeie K, Emoto Y, Yamaguchi M, Yasuda T, et al. Cardiac dysfunction and long-term prognosis in patients with nonobstructive hypertrophic cardiomyopathy and abnormal (123)I-15-(*p*-Iodophenyl)-3(*R,S*)-methylpentadecanoic acid myocardial scintigraphy. *Cardiology* 2000; 93: 43–49.
18. Hashimoto Y, Yamabe H, Yokoyama M. Myocardial defect detected by ^{123}I-BMIPP scintigraphy and left ventricular dysfunction in patients with idiopathic dilated cardiomyopathy. *Ann Nucl Med* 1996; 10: 225–230.
19. Kobayashi H, Nakata T, Han S, Takahashi N, Hashimoto A, Tsuchihashi K, et al. Fatty acid metabolic and perfusion abnormalities in hypertrophied myocardium assessed by dual tracer tomography using thallium-201 and iodine-123-beta-methylpentadecanoic acid. *J Cardiol* 1994; 24: 35–43.
20. Stevenson LW. Diseases of the myocardium. In: Bennette JC, Plum F, eds. *Cecel Textbook of Medicine*. Philadelphia, PA; W.B. Saunders, 1996: 327–336.
21. Fujibayashi Y, Nohara R, Hosokawa R, Okuda K, Yonekura Y, Tamaki N, et al. Metabolism and kinetics of iodine-123-BMIPP in canine myocardium. *J Nucl Med* 1996; 37: 757–761.
22. Matsunari I, Ichiyanagi K, Taki J, Nakajima K, Nishikawa T, Tonami N, et al. Quantitative analysis of ^{123}I-BMIPP imaging in relation to exercise-redistribution ^{201}Tl in patients with old myocardial infarction. *KAKU IGAKU (Jpn J Nucl Med)* 1994; 31: 927–933.
23. Yamamichi Y, Kusuoka H, Morishita K, Shirakami Y, Kurami M, Okano K, et al. Metabolism of iodine-123-BMIPP in perfused rat hearts. *J Nucl Med* 1995; 36: 1043–1050.
24. Knapp FF Jr, Ambrose KR, Goodman MM. New radioiodinated methyl-branched fatty acids for cardiac studies. *Eur J Nucl Med* 1986; 12 Suppl: S39–44.
25. Yoshida S, Ito M, Mitsunami K, Kinoshita M. Improved myocardial fatty acid metabolism after coronary angioplasty in chronic coronary artery disease. *J Nucl Med* 1998; 39: 933–938.
26. Arbab AS, Koizumi K, Toyama K, Arai T, Araki T. Technetium-99m-tetrofosmin, technetium-99m-MIBI and thallium-201 uptake in rat myocardial cells. *J Nucl Med* 1998; 39: 266–271.
27. Platts EA, North TL, Pickett RD, Kelly JD. Mechanism of uptake of technetium-tetrofosmin. I: Uptake into isolated adult rat ventricular myocytes and subcellular localization. *J Nucl Cardiol* 1995; 2: 317–326.
28. Sinusas AJ, Shi Q, Saltzberg MT, Vitols P, Jain D, Wackers FJ, et al. Technetium-99m-tetrofosmin to assess myocardial blood flow: experimental validation in an intact canine model of ischemia. *J Nucl Med* 1994; 35: 664–671.
29. Meleca MJ, McGoron AJ, Gerson MC, Millard RW, Gabel M, Biniakiewicz D, et al. Flow versus uptake comparisons of thallium-201 with technetium-99m perfusion tracers in a canine model of myocardial ischemia. *J Nucl Med* 1997; 38: 1847–1856.
30. Schaefer WM, Nowak B, Kaiser HJ, Koch KC, Block S, vom Dahl J, et al. Comparison of microsphere-equivalent blood flow (^{15}O-water PET) and relative perfusion (^{99m}Tc-tetrofosmin SPECT) in myocardium showing metabolism-perfusion mismatch. *J Nucl Med* 2003; 44: 33–39.
31. Merlet P, Valette H, Dubois-Rande JL, Moyse D, Duboc D, Dove P, et al. Prognostic value of cardiac metaiodobenzylguanidine imaging in patients with heart failure. *J Nucl Med* 1992; 33: 471–477.